European Journal of Medicinal Chemistry 112 (2016) 164–170

Contents lists available at ScienceDirect

European Journal of Medicinal Chemistry

journal homepage: http://www.elsevier.com/locate/ejmech

Short communication

The natural diterpene tonantzitlolone A and its synthetic enantiomer inhibit cell proliferation and kinesin-5 function

Tobias J. Pfeffer [a, 1], Florenz Sasse [b], Christoph F. Schmidt [c], Stefan Lakämper [c, 2], Andreas Kirschning [d], Tim Scholz [a, *]

[a] Molecular and Cell Physiology, Hannover Medical School (MHH), Carl-Neuberg-Str. 1, D-30625 Hannover, Germany
[b] Chemical Biology, Helmholtz Centre for Infection Research (HZI), Inhoffenstraße 7, D-38124 Braunschweig, Germany
[c] Drittes Physikalisches Institut, Georg-August University Göttingen, Friedrich-Hund-Platz 1, D-37077 Göttingen, Germany
[d] Institute of Organic Chemistry and Center of Biomolecular Drug Research (BMWZ), Leibniz University Hannover, Schneiderberg 1B, D-30167 Hannover, Germany

ARTICLE INFO

Article history:
Received 13 November 2015
Received in revised form
5 February 2016
Accepted 7 February 2016
Available online 8 February 2016

Keywords:
Inhibitor
Cytostatic
Diterpene
Kinesin spindle protein
Monoaster
Cancer

ABSTRACT

Tonantzitlolone A, a diterpene isolated from the Mexican plant *Stillingia sanguinolenta*, shows cytostatic activity. Both the natural product tonantzitlolone A and its synthetic enantiomer induce monoastral spindle formation in cell experiments which indicates inhibitory activity on kinesin-5 mitotic motor molecules. These inhibitory effects on kinesin-5 could be verified in *in vitro* single-molecule motility assays, where both tonantzitlolones interfered with kinesin-5 binding to its cellular interaction partner microtubules in a concentration-dependent manner, yet with a larger effect of the synthetic enantiomer. In contrast to kinesin-5 inhibition, both tonantzitlolone A enantiomers did not affect conventional kinesin-1 function; hence tonantzitlolones are not unspecific kinesin inhibitors. The observed stronger inhibitory effect of the synthetic enantiomer demonstrates the possibility to enhance the overall moderate anti-proliferative effect of the lead compound tonantzitlolon A by chemical modification.

1. Introduction

The endemic Mexican medical plant *Stillingia sanguinolenta* is particularly rich of unusual cyclic organic compounds [1,2]. For example, the two diterpenes tonantzitlolone A (**1**) and B (**2**; OAc at C-4′ of side chain) are secondary metabolites from *S. sanguinolenta*. Although diterpene cyclases commonly provide diterpenes with 14-membered rings, the backbone of tonantzitlolone A and B is based on a rare 15-membered flexibilane skeleton (**3**) (Fig. 1) [1,2]. It is known that plants of the genus *Stillingia*, which covers about 30 species mainly in the Americas, served natives for various medicinal purposes. For example, the roots of *S. sanguinolenta* are used in poultices after childbirth, and northern Mexican natives recommend infusions of leaves for the treatment of pulmonary ailments. Indian tribes of Navajos and Creek used the closely related *S. sylvatica* in a similar fashion [3,4]. So far, only initial reports appeared on the biological activity of these tonatzitlolones [5,6]. Here we disclose our preliminary findings on the biological anti-proliferative activity of tonantzitlolone A (**1**) and its synthetic enantiomer (*ent*)-tonantzitlolone A (**4**) as inhibitors of the mitotic motor protein kinesin-5 using a single-molecule fluorescence approach.

2. Results and discussion

Tonantzitlolone A (**1**) used in these studies was isolated from *Stillingia sanguinolenta* as reported previously [1] and described in the experimental section while its enantiomer (**4**) was obtained by total synthesis [5,7,8]. As judged by HPLC and ^{1}H NMR spectroscopy the purities were determined to be >95%, respectively. For a first biological evaluation both compounds were subjected to *in vitro* biological testing of their anti-proliferative activity on different mammalian cell lines. This biological evaluation indicated moderate low-μM activity. The results from these tests are given as values for the half-maximal cell growth inhibitory concentration (GI_{50},

* Corresponding author.
E-mail address: scholz.tim@mh-hannover.de (T. Scholz).
[1] Present address: Dept. of Cardiology and Angiology, Hannover Medical School, Carl-Neuberg-Str. 1, D-30625 Hannover, Germany.
[2] Present address: Institute for Mechanical Systems, D-MAVT, ETH Zurich, Tannenstrasse 3, CH-8092 Zurich, Switzerland.

http://dx.doi.org/10.1016/j.ejmech.2016.02.022
0223-5234/

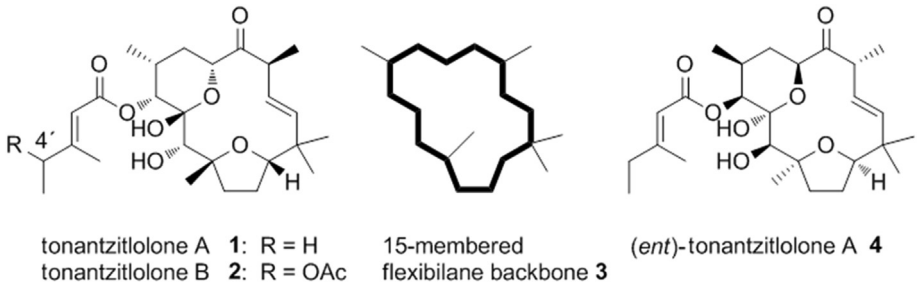

Fig. 1. Structures of tonantzitlolone A (**1**) and B (**2**), (*ent*)-tonantzitlolone A (**4**) and schematic representation of the flexibilane backbone (**3**).

Table 1).

Although both tonantzitlolone A enantiomers demonstrated an anti-proliferative impact on cell lines with GI_{50} values ranging from ~5 to 50 μM, from those cell experiments the origin of this cytostatic effect of tonantzitlolone A (**1**) and its enantiomer (**4**) and their cellular targets remained unclear. Very recently, the natural compound tonantzitlolone A (**1**) has been reported to activate PKC-theta and the heat shock factor 1 (HSF1) transcription factor in low-μM concentrations (~1–5 μM) and predominantly in renal carcinoma cells, thus starving these cells of glucose and causing cell death [6]. However, in addition to the anti-proliferative activity of tonantzitlolone A (**1**) we observed that when PtK_2 potoroo kidney cells were incubated for 18 h with 21.5 μM of **1** dissolved in methanol, ~20% of mitotic cells were arrested in mitosis and showed an unphysiological monoastral half spindle (Fig. 2B) instead of a normal bipolar spindle apparatus (Fig. 2A). In contrast, phenotypes of interphase cells were not affected by tonantzitlolone A (**1**), and cells incubated with only the solvent behaved regularly (Fig. 2). Such monoastral phenotype has been associated before with the inhibition of the molecular motor kinesin-5 (also known as Kif11, Eg5 or kinesin spindle protein) [9]. Thus, the observation of monoastral half-spindle formation suggests the motor protein kinesin-5 as one cellular target of tonantzitlolone A.

Members of the kinesin superfamily of motor proteins convert the chemical energy derived from ATP hydrolysis into directed movement along their cytoskeletal microtubule tracks. Microtubules are key structural elements of the spindle, and kinesin-5 is a mitotic motor protein which is required to generate the spindle's bipolar architecture thus playing an essential role in proper spindle morphogenesis [10,11]. This implies that kinesin-5 is also important for tumor formation. In mitosis, homotetrameric plus-end directed kinesin-5 molecules cross-link and simultaneously move antiparallel interpolar spindle microtubules [12–14], which results in outward-directed relative microtubule sliding and spindle pole separation [15]. While tubulin-derived microtubules are needed for multiple essential processes also in post-mitotic cells, kinesin motors that function almost exclusively during mitosis have recently emerged as a drugable target class in cancer chemotherapy [16], making small molecule inhibitors of kinesin-5 rational alternatives to tubulin targeting anti-cancer drugs.

To directly test for possible inhibitory effects of **1** and its synthetic enantiomer **4** on kinesin-5 function we used a single-molecule Total Internal Refection Fluorescence (TIRF) microscopy approach [17,18] (Fig. 3A) comparable to previous studies on kinesin-5 inhibition by monastrol [19]. We made use of a chimeric kinesin-5 motor construct as a model system for kinesin-5 function, in which the catalytic motor domain of kinesin-5 was fused to the truncated neck coiled coil of kinesin-1. This dimeric construct was reported to be very suitable for such studies as it was found to be fully functional and capable of long processive runs along microtubules, yet without the complex tetrameric structure of kinesin-5 and its associated tail-mediated self-inhibition [19,20]. In contrast to other inhibitor tests like kinesin-5 ATPase measurements or cell-based screening assays, single-molecule experiments can be performed with very little material in extremely small volumes of less than 5 μl. This can be important when only very limited sample sizes e.g. from total syntheses are available. In such single-molecule motility experiments, individual fluorescently labeled motor molecules are visualized and tracked while they proceed under ATP consumption along immobilized microtubules. From such experiments, functional parameters such as speed of movement or kinesin-5 microtubule binding frequency can be determined, parameters which are not accessible in cell screening or ATPase measurements. To visualize directed motion of individual kinesin molecules along microtubules, so-called kymographs, i.e. time plots of fluorescent kinesin positions on a microtubule, are often used (Fig. 3B). While static molecules appear as vertical traces, trajectories of kinesin molecules moving directed along the microtubule deviate towards one microtubule end to which the kinesin molecule moves. The velocity can be extracted from the slope of the respective trajectory.

Both enantiomers of tonantzitlolone A inhibit kinesin-5 molecules in a dose-dependent manner (Fig. 4, Fig. S1, Tables S1 and S2). While kinesin-5 velocity (Fig. 4A) and the fraction of motile kinesin-5 molecules (Fig. S1A) were unaffected, the attachment frequency of kinesin-5 to microtubules (Fig. 4B) as well as the total number of kinesin molecules bound per micrometer microtubule length (Fig. S1B) were significantly reduced with increasing inhibitor concentrations. The attachment frequency represents the binding affinity of kinesin to microtubules and is described by the number of kinesin molecules which landed and started moving on a microtubule per micrometer microtubule length per second time [21]. Tonantzitlolone A reduced the attachment of kinesin-5 molecules to microtubules with a half maximal inhibitory effect at IC_{50} ~147 μM. In comparison, the synthetic enantiomer **4** showed a stronger inhibitory effect than the natural compound **1**. The presence of (*ent*)-tonantzitlolone A had a more than three-fold stronger inhibitory effect on kinesin-5 binding to microtubules with a half maximal inhibitory effect at IC_{50} ~44.5 μM.

While the attachment frequency of kinesin-5 to microtubules is related to the attachment rate constant k_{on}, the total number of kinesin-5 molecules on microtubules, which additionally includes

Table 1
Half-maximal anti-proliferative concentrations GI_{50} [μM] of **1** and **4** with cultured mammalian cell lines. Values shown are means of two determinations in parallel; U-937 (human histiocytic lymphoma), L-929 (mouse fibroblasts), PtK_2 (potoroo kidney cells); n.d., not determined.

Compound	U-937	L-929	PtK_2
1	45 ± 15	>80	43 ± 6
4	4.5 ± 1.9	37 ± 6	n.d.

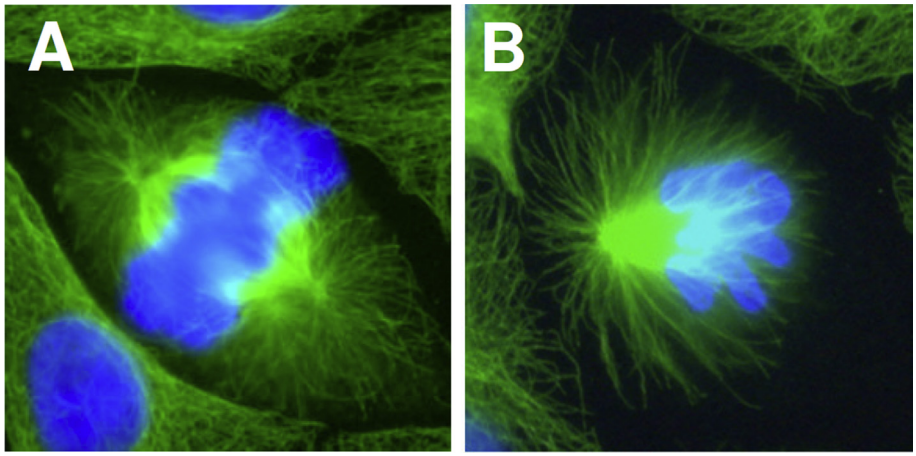

Fig. 2. Effect of tonantzitlolone A on mitotic cells. Microtubules are shown in green, DAPI labeled DNA is shown in blue. (A) PtK_2 potoroo kidney cells with a mitotic cell in the centre which formed a regular bipolar spindle apparatus. (B) After incubation of PtK_2 potoroo cells with 21.5 μM tonantzitlolone A for 18 h in ~20% of mitotic cells monoastral half-spindles could be observed. (For interpretation of the references to colour in this figure legend, the reader is referred to the web version of this article.)

stationary as well as moving kinesin-5 molecules present already at the beginning of recordings, is related to the ratio of k_{on} and the dissociation rate constant k_{off} (Fig. 5A). Furthermore, k_{off} directly influences the run length of kinesin molecules as faster dissociation leads to shorter traveling distances. Under the experimental conditions used in this study, however, the duration of processive runs of kinesin-5 molecules usually exceeded the already extended observation times (e.g. Fig. 3B) both in the absence and the presence of inhibitors. Hence, k_{off} could not have been increased dramatically by tonantzitlolone A or (*ent*)-tonantzitlolone A. As mentioned above, the total number of kinesin-5 molecules per micrometer microtubule length, i.e. the ratio k_{on}/k_{off}, was significantly reduced with increasing concentrations of tonantzitlolone A (**1**) or (*ent*)-tonantzitlolone A (**4**) (Fig. S1B). With IC_{50} values of ~175 and ~54 μM, respectively, the concentration-dependent decrease showed a behaviour almost similar to the attachment frequency. The observed reduction of the total number of kinesin molecules per micrometer microtubule length could therefore be a result of a respective reduction in k_{on}. Together with the observation that no decrease in the run length, i.e. k_{off}, could be observed in the presence of both tonantzitlolones, this suggests a possible model in which tonantzitlolone A (**1**) and (*ent*)-tonantzitlolone A (**4**) reduce initial attachment of kinesin-5 molecules to microtubules while dissociation is not enhanced (Fig. 5B).

An undiminished velocity of individual kinesin-5 molecules in the presence of the well-characterized kinesin-5 inhibitor monastrol has been reported before in combination with an increase in kinesin detachment from microtubules [19]. In multi-molecule kinesin motility assays, on the other hand, increasing concentrations of monastrol caused a (sometimes very abrupt) decrease in microtubule gliding velocity with IC_{50} values of ~14–240 μM [9,19], which has also been observed for the inhibitor Terpendole E [22]. For an individual kinesin-5 molecule, microtubule-stimulated ATPase might be unaffected by Tonantzitlolone A inhibitors as single-molecule velocity remained unchanged even at high inhibitor concentrations. In ensemble ATPase measurements, however, an increasing number of non-active kinesin molecules clogged by increasing inhibitor concentrations would feign an overall decrease in ATPase activity. The observation that the attachment frequency of kinesin-5 molecules decreased with increasing inhibitor concentrations suggests that tonantzitlolone A and its synthetic enantiomer lock kinesin-5 molecules in an ADP-containing or ADP-like conformation with low microtubule affinity. This might cause immediate release of the kinesin motor molecule from the microtubule and prevent initiation of processive movement.

Current models for allosteric kinesin-5 inhibition by small molecules involve competition with the energy substrate ATP [23–25] and disturbance of microtubule binding and microtubule-stimulated ATPase activity as a result of kinesin conformational changes in response to inhibitor binding [26–28]. Many reported kinesin-5 inhibitors such as monastrol, ispinesib and *S*-trityl-L-cysteine target a surface-exposed allosteric inhibitor binding pocket, which is remote from the nucleotide binding site and mainly comprises loop-5 of kinesin-5 molecules and adjacent residues of helix-3 [28–32]. Loop-5 is a key structural element found in all kinesins but is longest in the mitotic kinesin-5, and it was suggested to function there as an on/off switch which can interact with the nucleotide binding site [33,34]. Although both enantiomers of tonantzitlolone A are chemically identical with respect to their 15-membered flexibilane backbone and functional groups, the stronger inhibition of kinesin-5 by (*ent*)-tonantzitlolone A (**4**) suggests stronger binding to kinesin-5 and/or higher inhibition efficiency. Such stereochemical aspects have been reported before to have an impact on the potency of kinesin-5 inhibitors [9,29,32,35]. Hydrophobic interactions of the inhibitor with the core of the kinesin-5 motor were suggested to be essential for binding affinity and biological activity, and increased binding affinity and therefore increased biological activity was explained by additional binding of the inhibitor to a cooperative minor binding pocket [29]. The higher inhibition potency of (*ent*)-tonantzitlolone A (**4**) could be a hint that the absolute structure of the synthetic enantiomer **4** might fit better into the allosteric inhibitor binding pocket of kinesin-5. Rare cases have been reported where both enantiomers exhibited similar biological activities. Wiskostatin, a small molecule that inhibits activation of Arp2/3 by N-WASP and therefore actin-polymerization is such an example. The (*S*)-isomer shows an IC_{50} value of 4.35 μM and (*R*)-wiskostatin an IC_{50} value of 3.44 μM [36].

For a possible future therapeutic use of tonantzitlolone A derivates it is necessary to screen for unwanted side effects on other kinesin family motor proteins such as neuronal kinesin-1. To test if tonantzitlolone A and (*ent*)-tonantzitlolone A (**4**) selectively inhibit kinesin-5, the motile behaviour of kinesin-1 molecules in the presence of these inhibitors was measured (Fig. 4, open symbols). Both velocity and microtubule attachment frequency of kinesin-1 molecules remained unchanged in the presence of **1** and **4**, and

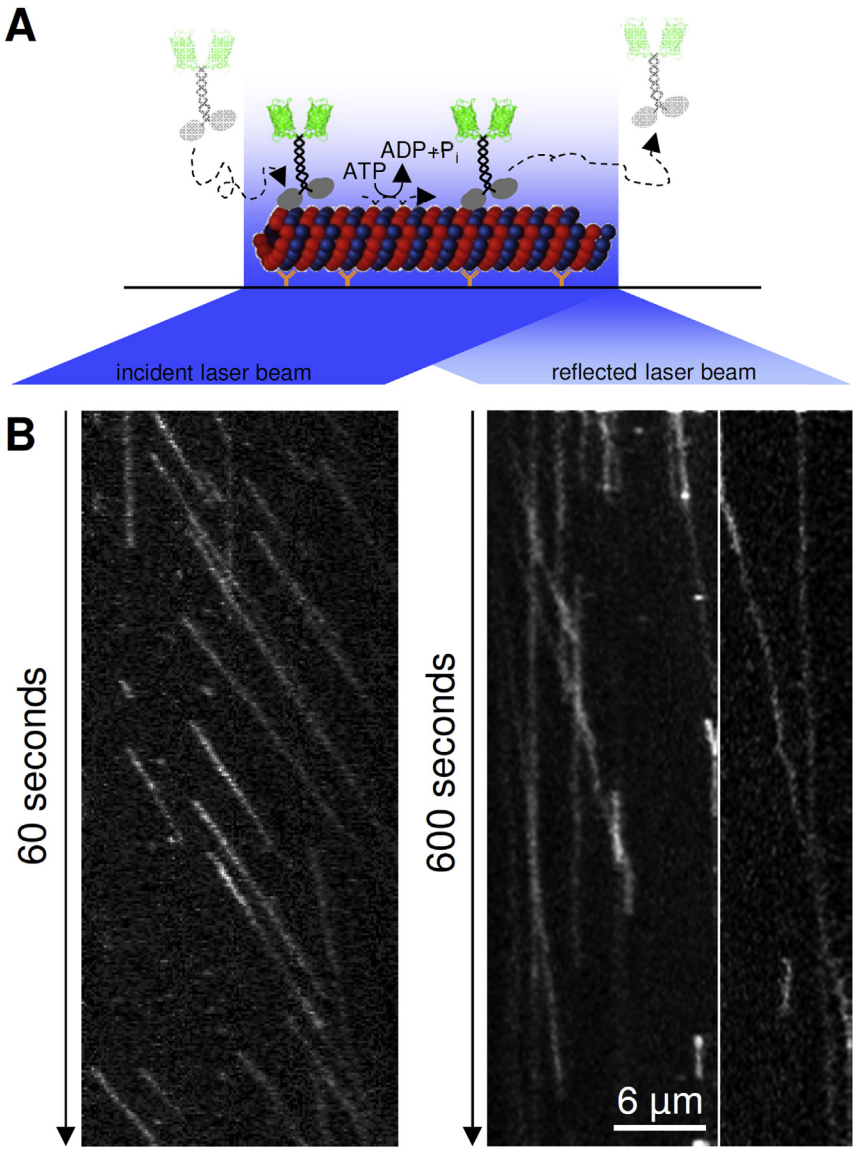

Fig. 3. *In vitro* kinesin-1 and kinesin-5 single-molecule motility assays (A) Experimental arrangement (not to scale): GFP-tagged (green) kinesin molecules land on and move along fluorescently Cy5-labeled microtubules (alpha-tubulin red and beta-tubulin dark blue) immobilized on a glass surface of a flow chamber by anti-tubulin antibodies (orange). Evanescent field illumination (blue rays) allows single molecule detection. (B) Kymographs, time plots of fluorescent kinesin positions on a microtubule, of GFP-tagged kinesin-1 (left) and GFP-tagged kinesin-5 molecules (right, two examples) moving along immobilized microtubules in the presence of 1 mM ATP. The velocity of a molecule can be extracted from the slope of the respective trajectory. (For interpretation of the references to colour in this figure legend, the reader is referred to the web version of this article.)

immobile kinesin-1 molecules did not occur more often (Fig. S1A). This suggests that (i) these tonantzitlolones inhibit kinesin-5 but not kinesin-1 function and therefore are not general inhibitors for kinesin motors and that (ii) these tonantzitlolones do not act as kinesin-5 inhibitors via binding to the microtubule track which would affect both kinesin-1 [18] and kinesin-5. However, it was reported previously that another mitotic kinesin family member, class-7 kinesin centromere-associated protein-E (CENP-E), can be curbed by loop-5 directed allosteric inhibition [37], yet with a different cellular phenotype of failing metaphase chromosome alignment. Therefore, the impact of tonantzitlolone A on other kinesin family members such as kinesin-7 needs to be tested, although kinesin-7 inhibition would also result in the aspired mitotic arrest of tumor cells.

Sometimes, drugs characterized in *in vitro* inhibition assays do not - or only to a small extent - show biological activity in cell-based experiments because they cannot pass the cell membrane of tumor cells [38] or are eliminated from the cells by the activity of the multidrug resistance (MDR) [35]. Since single-molecule *in vitro* as well as cell growth experiments showed kinesin-5 inhibition, both tonantzitlolones seem to be membrane permeable and are active in cells.

3. Conclusions

The mitotic molecular motor protein kinesin-5 was reported to be a rational target of drug discovery in cancer chemotherapy. In addition to tonantzitlolone A's recently reported cytotoxic effects based on PKC-theta and HSF1 transcription factor activation [6], our results from cell biological and single-molecule motility studies show that the natural compound tonantzitlolone A (**1**) and its synthetic enantiomer (*ent*)-tonantzitlolone A (**4**) are novel membrane permeable inhibitors of kinesin-5 with anti-proliferative activity. Kinesin-5 inhibition by the latter one was stronger, while

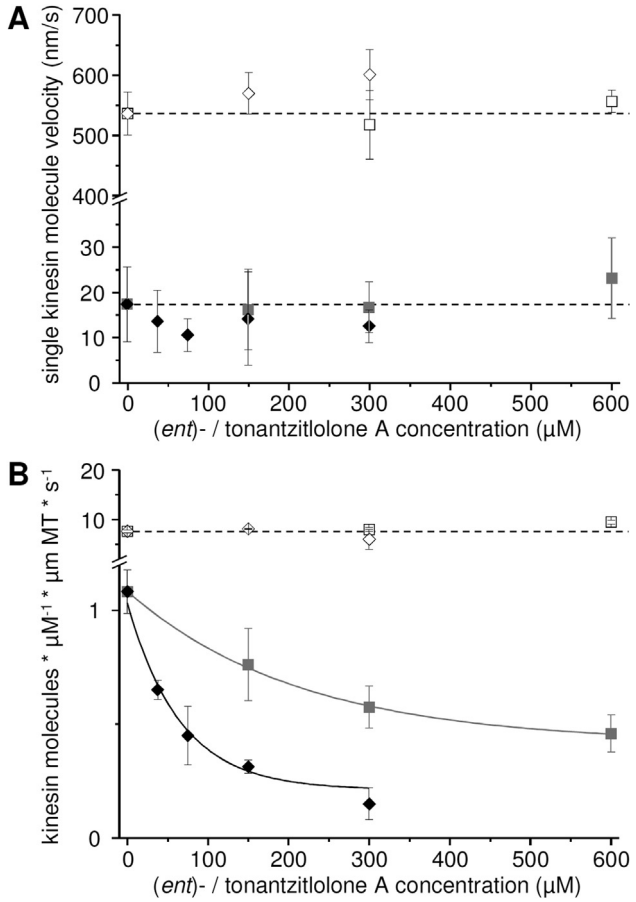

Fig. 4. Tonantzitlolone A (**1**, square symbols) and (*ent*)-tonantzitlolone A (**4**, diamond symbols) effects on kinesin-1 (open symbols) and kinesin-5 (solid symbols) motile properties. Error bars represent SEM of individual experiments. Detailed values are given in Tables S1 and S2. (A) Single-molecule velocity of kinesin-1 and kinesin-5 molecules did not change with increasing concentrations of both tonantzitlolones. Value levels found in solvent DMSO controls but in the absence of inhibitors are depicted as horizontal dashed lines both for kinesin-1 and kinesin-5. (B) The attachment frequency of kinesin-5 molecules, i.e. the number of kinesin molecules which landed on a microtubule and started moving per micrometer microtubule stretch and second, decreased exponentially (light and dark gray fits) with increasing concentrations of both tonantzitlolone A enantiomers while kinesin-1 was not affected. The attachment frequency of kinesin-1 observed in solvent DMSO controls but in the absence of inhibitors is depicted as horizontal dashed line.

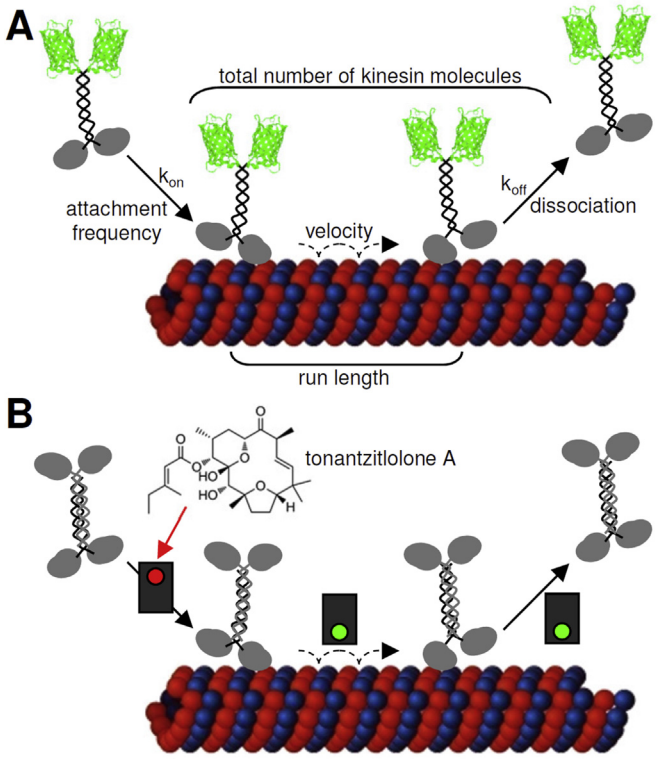

Fig. 5. Functional parameters of individual kinesin-5 molecules (A) and a possible mechanism for tonantzitlolone inhibitory effects on kinesin-5 (B). Tonantzitlolone A (**1**) and (*ent*)-tonantzitlolone A (**4**) inhibit initial attachment of kinesin-5 molecules to microtubules while dissociation is not enhanced and speed of movement not reduced.

both enantiomeric diterpenes **1** and **4** did not inhibit neuronal kinesin-1, another member of the kinesin superfamily. The exact mechanism by which these tonantzitlolones inhibit kinesin-5 as well as their binding site within kinesin-5 molecules need to be characterized in future studies. To increase the overall moderate inhibitor potency of this novel natural-compound based kinesin-5 inhibitors diversely functionalized tonantzitlolone derivatives could be produced by semi- and total synthesis and characterized by crystallographic and *in silico* inhibitor docking [29,30,39] and functional *in vitro* and cell activity studies.

4. Experimental

4.1. Tonantzitlolone preparation and characterization

Tonantzitlolone A (**1**) was extracted from the endemic Mexican medical plant *Stillingia sanguinolenta* as reported previously [1,7]. *S. sanguinolenta* plant material was collected in Valle Alto, Monterrey N.L., Mexico in May 1990 and March 1992 by J. Jakupovic. A herbarium specimen is deposited at the Monterrey Institute of Technology and Higher Education (ITESM) Herbarium (ID 8482).

800 g air dried *S. sanguinolenta* roots were extracted over night with a combination of petroleum ether, methyl *tert*-butyl ether, and methanol. After evaporation of the solvent, 35 g extract were dissolved in methanol and kept at −20 °C over night. The soluble part (24 g) was separated into 10 fractions by column chromatography using mixes of petroleum ether, ethyl acetate, and methanol with increasing polarity. Fractions 1, 2, 4, 8, 9 and 10 were discarded, while fraction 3 was further separated by HPLC (RP 8; 8 × 250 mm) to yield 1 mg of tonantzitlolone A (methanol/H_2O = 9:1, R_t 8.3 min).

S. sanguinolenta aerial parts were treated in the same manner as described above yielding 31 g of extract from 800 g starting material. This extract was separated by column chromatography with mixtures comprising petroleum ether, methyl *tert*-butyl ether, and methanol to furnish eight fractions. Fractions 1, 7 and 8 were discarded. HPLC of fraction 2 separated 15 mg of tonantzitlolone A (R_f 0.35) from other *S. sanguinolenta* compounds such as cembrene A and kauranes as additionally evaluated by thin layer chromatography (petroleum ether/methyl *tert*-butyl ether = 9:1) as published previously [1]. The optical rotation for purified tonantzitlolone A was $[\alpha]_D^{20} = +134°$ ($CHCl_3$; *c* 0.25), and spectroscopic data (see supporting information) were as reported previously [1]: IR ν_{max} (KBr) cm^{-1}: 3381, 1741, 1684; Electron ionization mass spectrometry (EIMS) (probe, 70 eV) *m/z* (relative intensities): 464.2774 (2) $[M]^+$ (calculated for $C_{26}H_{40}O_7$: 464.2774), 446 $[M - H_2O]^+$ (6), 350, $[M\text{-}RCOOH]^+$ (2), 332 $[350\text{-}H_2O]^+$ (1), 304, $[332\text{-}CO]^+$ (1), 245 (5), 180 (6), 97 $[RCO]^+$ (100). Tonantzitlolone A (**1**), stored in the refrigerator at 4 °C, is stable for several years.

The synthetic enantiomer (*ent*)-tonantzitlolone A (**4**) was produced by total synthesis and purified by column chromatography

(hexane/ethyl acetate = 2:1) as previously described in detail [5,7,8] (see also supporting information). Optical rotation for (*ent*)-tonantzitlolone A was determined to be $[\alpha]_D^{20} = -119^\circ$ (*c* 0.06, $CHCl_3$). Apart from this difference all spectroscopic data (NMR, IR, MS) (see also supporting information) were in full accordance with those of the plant extracted authentic material (see above) [5,7].

4.2. Cellular proliferation assays

3-(4,5-Dimethylthiazol-2-yl)-2,5-diphenyltetrazolium bromide (MTT) was used to measure growth and viability of cells which are capable of reducing it to a violet formazan product. 60 μL of serial dilutions of the test compounds were added to 120 μL aliquots of a cell suspension (50,000/mL) in 96-well microplates. Blank and solvent controls were incubated under identical conditions for 5 d. 20 μL MTT in phosphate buffered saline (PBS) were added to give a final concentration of 0.5 mg/ml. After 2 h, the precipitate of formazan crystals was centrifuged, and the supernatant discarded. The precipitate was washed with PBS (100 μL) and dissolved in isopropanol containing 0.4% hydrochloric acid (100 μL). The microplates were gently shaken for 20 min to ensure a complete dissolution of the formazan and finally measured at 595 nm using an ELISA plate reader. All experiments were carried out in two parallel experiments. Activity values were calculated as the mean with respect the controls set to 100%.

4.3. Fluorescence staining

PtK_2 cells (ATCC CCL-56) were grown on glass coverslips (13 mm diameter) in four-well plates. Exponentially growing cells were incubated with the compounds for 18 h. Cells were fixed with cold (−20 °C) acetone-methanol (1:1) for 10 min. For labeling of microtubules, cells were first incubated with a mouse antibody against α-tubulin (1:500; Sigma), then with a secondary goat anti-mouse IgG antibody conjugated with Alexa Fluor 488 (1:200; Molecular Probes) at 37 °C for 45 min. The nuclei and chromosomes were stained with DAPI (1 μg/ml). The cells were washed with PBS between different incubations. The coverslips were mounted using Prolong Antifade (Molecular Probes), and viewed with a Zeiss Axiophot fluorescence microscope using appropriate filter sets.

4.4. Single-molecule TIRF microscopy

Motility assays of single eGFP-tagged rat kinesin-1 [18] or kinesin-5/kin-1 chimera molecules [19] along immobilized paclitaxel-stabilized Cy5-labeled microtubules (MTs) [17,18] were performed at 23 °C in buffer BRB12 (12 mM PIPES, 1 mM $MgCl_2$, 1 mM EGTA, 10 mg/ml glucose, pH 6.8) supplemented with 10 μM paclitaxel and 1 mM ATP in the presence of different inhibitor concentrations. MTs and kinesin molecules were excited by a HeNe laser (633 nm, 35 mW, Coherent, CA, USA) and a 473 nm DPSS laser (MBL 473, 100 mW, HB-Laserkomponenten, Schwaebisch Gmünd, Germany), respectively, and their positions detected using a self-made objective type total internal reflection fluorescence (TIRF) microscope with single-fluorophore sensitivity [18]. To minimize photo damage of proteins or bleaching of fluorophores the assay buffers were supplemented with an oxygen scavenger system (10 mg/ml glucose, 50 U/ml glucose oxidase, 7600 U/ml catalase, and 10 mM DTT). Additionally, 50 μs laser pulses interrupted by 450 μs pauses were used to excite the fluorescently labeled samples. After incubation for 7 min with different concentrations of potential inhibitors or their solvent DMSO movement of fluorescently labeled kinesin-1 molecules was recorded for time periods of 60 s with 5 frames per second while for the slower kinesin-5 movement time periods of 600 s and frame rates of 0.5 per second were used.

For analysis individual fluorescently labeled molecules were located and tracked basically as described previously using the computer program ImageJ (W.S. Rasband, NIH, Bethesda, MD), the plug-in Multiple Kymograph [21] and the macro ListSelectionCoordinates.

Conflict of interest

The authors declare no conflict of interest.

Acknowledgement

We are grateful to AnalytiCon Discovery (Potsdam, Germany) for an authentic sample of tonantzitlolone A. The total synthesis of (*ent*)-tonantzitlolone A was achieved by Dr. C. Jasper for which we are thankful. We thank P. Uta, B. Hinkelmann and T. Beier for excellent technical assistance and J. Pliquet, D.J. Manstein and B. Brenner for helpful discussions.

Appendix A. Supplementary data

Supplementary data related to this article can be found at http://dx.doi.org/10.1016/j.ejmech.2016.02.022.

References

[1] G. Dräger, F. Jeske, E. Kunst, E.G. Lopez, H.V. Sanchez, F. Tsichritzis, A. Kirschning, J. Jakupovic, Tonantzitlolone and other diterpenes from Stillingia sanguinolenta, Eur. J. Org. Chem. (2007) 5020–5026.
[2] T. Busch, A. Kirschning, Recent advances in the total synthesis of pharmaceutically relevant diterpenes, Nat. Prod. Rep. 25 (2008) 318–341.
[3] C.F. Millspaugh, American Medicinal Plants, Dover Publications Inc, New York, 1974, p. 811.
[4] D.E. Moerman, Medicinal Plants of Native America, University of Michigan, Museum of Antropology, Ann Arbor, 1986, p. 910.
[5] C. Jasper, A. Adibekian, T. Busch, M. Quitschalle, R. Wittenberg, A. Kirschning, Total synthesis of cyclic diterpene tonantzitlolone based on a highly stereoselective substrate-controlled aldol reaction and ring-closing metathesis, Chem. Eur. J. 12 (2006) 8719–8734.
[6] C. Sourbier, B.T. Scroggins, P.Z. Mannes, P.J. Liao, K. Siems, D. Wolf, J.A. Beutler, W.M. Linehan, L. Neckers, Tonantzitlolone cytotoxicity toward renal cancer cells is PKCtheta- and HSF1-dependent, Oncotarget 6 (2015) 29963–29974.
[7] C. Jasper, R. Wittenberg, M. Quitschalle, J. Jakupovic, A. Kirschning, Total synthesis and elucidation of the absolute configuration of the diterpene tonantzitlolone, Org. Lett. 7 (2005) 479–482.
[8] R. Wittenberg, C. Beier, G. Dräger, G. Jas, C. Jasper, H. Monenschein, A. Kirschning, Towards the total synthesis of tonantzitlolone – preparation of key fragments and the complete carbon backbone, Tetrahedron Lett. 45 (2004) 4457–4460.
[9] T.U. Mayer, T.M. Kapoor, S.J. Haggarty, R.W. King, S.L. Schreiber, T.J. Mitchison, Small molecule inhibitor of mitotic spindle bipolarity identified in a phenotype-based screen, Science 286 (1999) 971–974.
[10] K.E. Sawin, K. LeGuellec, M. Philippe, T.J. Mitchison, Mitotic spindle organization by a plus-end-directed microtubule motor, Nature 359 (1992) 540–543.
[11] A. Castillo, H.C. Morse 3rd, V.L. Godfrey, R. Naeem, M.J. Justice, Overexpression of Eg5 causes genomic instability and tumor formation in mice, Cancer Res. 67 (2007) 10138–10147.
[12] L.C. Kapitein, B.H. Kwok, J.S. Weinger, C.F. Schmidt, T.M. Kapoor, E.J. Peterman, Microtubule cross-linking triggers the directional motility of kinesin-5, J. Cell Biol. 182 (2008) 421–428.
[13] L.C. Kapitein, E.J. Peterman, B.H. Kwok, J.H. Kim, T.M. Kapoor, C.F. Schmidt, The bipolar mitotic kinesin Eg5 moves on both microtubules that it crosslinks, Nature 435 (2005) 114–118.
[14] M.T. Valentine, P.M. Fordyce, T.C. Krzysiak, S.P. Gilbert, S.M. Block, Individual dimers of the mitotic kinesin motor Eg5 step processively and support substantial loads in vitro, Nat. Cell Biol. 8 (2006) 470–476.
[15] B.H. Kwok, J.G. Yang, T.M. Kapoor, The rate of bipolar spindle assembly depends on the microtubule-gliding velocity of the mitotic kinesin Eg5, Curr. Biol. 14 (2004) 1783–1788.
[16] R. Sakowicz, J.T. Finer, C. Beraud, A. Crompton, E. Lewis, A. Fritsch, Y. Lee, J. Mak, R. Moody, R. Turincio, et al., Antitumor activity of a kinesin inhibitor, Cancer Res. 64 (2004) 3276–3280.
[17] M.H. Hinrichs, A. Jalal, B. Brenner, E. Mandelkow, S. Kumar, T. Scholz, Tau protein diffuses along the microtubule lattice, J. Biol. Chem. 287 (2012) 38559–38568.
[18] A. Rump, T. Scholz, C. Thiel, F.K. Hartmann, P. Uta, M.H. Hinrichs, M.H. Taft,

G. Tsiavaliaris, Myosin-1C associates with microtubules and stabilizes the mitotic spindle during cell division, J. Cell Sci. 124 (2011) 2521–2528.
[19] S. Lakämper, C. Thiede, A. Düselder, S. Reiter, M.J. Korneev, L.C. Kapitein, E.J. Peterman, C.F. Schmidt, The effect of monastrol on the processive motility of a dimeric kinesin-5 head/kinesin-1 stalk chimera, J. Mol. Biol. 399 (2010) 1–8.
[20] A. Düselder, C. Thiede, C.F. Schmidt, S. Lakämper, Neck-linker length dependence of processive Kinesin-5 motility, J. Mol. Biol. 423 (2012) 159–168.
[21] A. Seitz, H. Kojima, K. Oiwa, E.M. Mandelkow, Y.H. Song, E. Mandelkow, Single-molecule investigation of the interference between kinesin, tau and MAP2c, Embo J. 21 (2002) 4896–4905.
[22] J. Nakazawa, J. Yajima, T. Usui, M. Ueki, A. Takatsuki, M. Imoto, Y.Y. Toyoshima, H. Osada, A novel action of terpendole E on the motor activity of mitotic Kinesin Eg5, Chem. Biol. 10 (2003) 131–137.
[23] T. Takeuchi, S. Oishi, T. Watanabe, H. Ohno, J. Sawada, K. Matsuno, A. Asai, N. Asada, K. Kitaura, N. Fujii, Structure-activity relationships of carboline and carbazole derivatives as a novel class of ATP-competitive kinesin spindle protein inhibitors, J. Med. Chem. 54 (2011) 4839–4846.
[24] L. Luo, C.A. Parrish, N. Nevins, D.E. McNulty, A.M. Chaudhari, J.D. Carson, V. Sudakin, A.N. Shaw, R. Lehr, H. Zhao, et al., ATP-competitive inhibitors of the mitotic kinesin KSP that function via an allosteric mechanism, Nat. Chem. Biol. 3 (2007) 722–726.
[25] C.A. Parrish, N.D. Adams, K.R. Auger, J.L. Burgess, J.D. Carson, A.M. Chaudhari, R.A. Copeland, M.A. Diamond, C.A. Donatelli, K.J. Duffy, et al., Novel ATP-competitive kinesin spindle protein inhibitors, J. Med. Chem. 50 (2007) 4939–4952.
[26] Z. Maliga, T.M. Kapoor, T.J. Mitchison, Evidence that monastrol is an allosteric inhibitor of the mitotic kinesin Eg5, Chem. Biol. 9 (2002) 989–996.
[27] L. Luo, J.D. Carson, K.S. Molnar, S.J. Tuske, S.J. Coales, Y. Hamuro, C.M. Sung, V. Sudakin, K.R. Auger, D. Dhanak, et al., Conformation-dependent ligand regulation of ATP hydrolysis by human KSP: activation of basal hydrolysis and inhibition of microtubule-stimulated hydrolysis by a single, small molecule modulator, J. Am. Chem. Soc. 130 (2008) 7584–7591.
[28] H.Y. Kaan, J. Major, K. Tkocz, F. Kozielski, S.S. Rosenfeld, “Snapshots” of ispinesib-induced conformational changes in the mitotic kinesin Eg5, J. Biol. Chem. 288 (2013) 18588–18598.
[29] C. Jiang, Y. Chen, X. Wang, Q. You, Docking studies on kinesin spindle protein inhibitors: an important cooperative 'minor binding pocket' which increases the binding affinity significantly, J. Mol. Model 13 (2007) 987–992.
[30] H.Y. Kaan, J. Weiss, D. Menger, V. Ulaganathan, K. Tkocz, C. Laggner, F. Popowycz, B. Joseph, F. Kozielski, Structure-activity relationship and multidrug resistance study of new S-trityl-L-cysteine derivatives as inhibitors of Eg5, J. Med. Chem. 54 (2011) 1576–1586.
[31] E.D. Kim, R. Buckley, S. Learman, J. Richard, C. Parke, D.K. Worthylake, E.J. Wojcik, R.A. Walker, S. Kim, Allosteric drug discrimination is coupled to mechanochemical changes in the kinesin-5 motor core, J. Biol. Chem. 285 (2010) 18650–18661.
[32] I. Garcia-Saez, S. DeBonis, R. Lopez, F. Trucco, B. Rousseau, P. Thuery, F. Kozielski, Structure of human Eg5 in complex with a new monastrol-based inhibitor bound in the R configuration, J. Biol. Chem. 282 (2007) 9740–9747.
[33] T.D. Harrington, N. Naber, A.G. Larson, R. Cooke, S.E. Rice, E. Pate, Analysis of the interaction of the Eg5 Loop5 with the nucleotide site, J. Theor. Biol. 289 (2011) 107–115.
[34] J.S. Waitzman, A.G. Larson, J.C. Cochran, N. Naber, R. Cooke, F. Jon Kull, E. Pate, S.E. Rice, The loop 5 element structurally and kinetically coordinates dimers of the human kinesin-5, Eg5, Biophys. J. 101 (2011) 2760–2769.
[35] H.Y. Kaan, V. Ulaganathan, O. Rath, H. Prokopcova, D. Dallinger, C.O. Kappe, F. Kozielski, Structural basis for inhibition of Eg5 by dihydropyrimidines: stereoselectivity of antimitotic inhibitors enastron, dimethylenastron and fluorastrol, J. Med. Chem. 53 (2010) 5676–5683.
[36] J.R. Peterson, L.C. Bickford, D. Morgan, A.S. Kim, O. Ouerfelli, M.W. Kirschner, M.K. Rosen, Chemical inhibition of N-WASP by stabilization of a native autoinhibited conformation, Nat. Struct. Mol. Biol. 11 (2004) 747–755.
[37] K.W. Wood, L. Lad, L. Luo, X. Qian, S.D. Knight, N. Nevins, K. Brejc, D. Sutton, A.G. Gilmartin, P.R. Chua, et al., Antitumor activity of an allosteric inhibitor of centromere-associated protein-E, Proc. Natl. Acad. Sci. U. S. A. 107 (2010) 5839–5844.
[38] S. Oishi, T. Watanabe, J. Sawada, A. Asai, H. Ohno, N. Fujii, Kinesin spindle protein (KSP) inhibitors with 2,3-fused indole scaffolds, J. Med. Chem. 53 (2010) 5054–5058.
[39] S. Nagarajan, D.A. Skoufias, F. Kozielski, A.N. Pae, Receptor-ligand interaction-based virtual screening for novel Eg5/kinesin spindle protein inhibitors, J. Med. Chem. 55 (2012) 2561–2573.